

K. Balashev  
I. Panaiotov  
I. Petkov

# Interfacial photochemical tautomerization in polyacryloylacetone monolayers

Received: 9 March 1998  
Accepted: 29 May 1998

K. Balashev · Prof. Dr. I. Panaiotov (✉)  
Biophysical Chemistry Laboratory  
University of Sofia  
J. Bourchier Str. 1  
1126 Sofia  
Bulgaria

I. Petkov  
Department of Organic Chemistry  
University of Sofia  
J. Bourchier Str. 1  
1126 Sofia  
Bulgaria

**Abstract** The surface organization of the enol units of polyacryloylacetone (PAA) monolayer at the air–water interface is examined using surface pressure and surface potential measurements and theoretical calculations based on molecular models.

The mechanism and kinetics of the photochemical enol–keto tautomerization is studied by measuring the increase of the surface area at constant surface pressure. The effect is due to

the increase of the area per monomer units during the consecutive enol-to-keto photoconversion and slow interfacial reorganization of these forms to a more favorable state.

**Key words** Photochemical tautomerization – polyacryloylacetone monolayer – enol-to-keto photoconversion

## Introduction

Recently, the polymers containing  $\beta$ -dicarbonyl group ( $\beta$ -DCG), their derivatives and analogs have been intensively investigated [1–7]. Some of the reasons for this interest were:

- possible technological applications in photolithography, chemical lasers, energy storage devices at a molecular level, high-energy radiation detectors, polymer stabilizers and as chelating agents or sensor systems [5, 8];
- the study of the influence of radiation (UV-light,  $\gamma$ -rays, X-rays) on the properties of polymers containing  $\beta$ -DCG is relevant to numerous biological processes. In fact,  $\beta$ -DCG is a structural analog in many biologically important polymers [5]. A monolayer of polyacryloylacetone (PAA) at the air–water interface is a convenient simple model to study the mechanism of the photoinduced enol–keto tautomerization in organized molecular layers (Fig. 1).

In principle, the mechanism of a photochemical reaction strongly depends on the organization and orientation of the polymeric molecules at the interface.

By using pressure–area isotherms measurement, AFM imaging and a new rheological approach, we obtained information about the state and mechanical properties of the enol form of PAA monolayers [9, 10].

The influence of normal and basic pH of the subphase and the presence of  $\text{Cu}^{2+}$  ions on the properties of the enol form of PAA monolayers has been studied [9].

The role of the nature of the interface (dichloromethane–water or air–water interfaces) on the organization and dilatational properties of the enol form of PAA monolayers has also been investigated [10].

This paper has two purposes:

(i) to define more precisely the concept of surface organization of the enol form of a PAA-monolayer by using an additional information obtained from surface potential measurements and theoretical calculations based on molecular models.

(ii) to study the kinetics and mechanism of the photochemical enol–keto tautomerization at the air–water interface, on the basis of the suggestion that enol unit requires a smaller area than the keto unit of PAA monolayers and

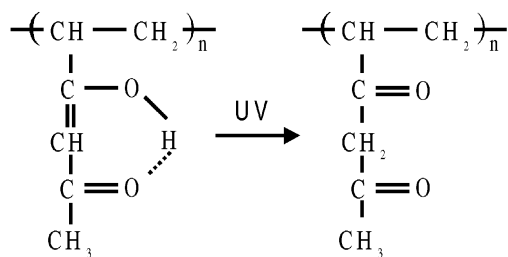


Fig. 1 Photochemical reaction of enol-keto tautomerization of polyacryloylacetone (PAA)

during the irradiation of the enol form of PAA monolayers the surface area increases.

## Materials and methods

### Polymers and solvents

Polyacryloylacetone (PAA) was obtained from the Department of Applied Chemistry, Technical College, University of Tokushima. According to [3], the molecular weight of PAA, determined by gel permeation chromatography is larger than 100 000. Chromatographically pure chloroform was used as a spreading solvent for PAA. The polymer was dissolved in chloroform to give a 0.5 mg/ml. Bidistilled water was used. The temperature of the subphase was controlled to be  $20 \pm 0.5^\circ\text{C}$ .

### Isotherm measurement of spread polymer monolayers

#### Surface pressure ( $\pi$ )-surface area ( $A$ ) isotherm measurements

PAA was spread by using an Exmire microsyringe on a water subphase (pH  $\sim 6$ ) on the entire area available ( $927\text{ cm}^2$ ). In order to avoid any doubts about the accuracy of the obtained results two methods of measuring the isotherms were applied. The first one was by using a Langmuir film balance and the second one was the Wilhelmy method with a platinum plate and a Beckman electrobalance LM 600 connected to a personal computer provided with an user software for real time data measurement. The values of surface pressure after spreading were less than  $0.2\text{ mN/m}$ . Monolayers were left for about 15 min before measurement. Surface pressure ( $\pi$ )-surface area ( $A$ ) isotherms were obtained by continuous compression of the spread monolayers at constant rate,  $U_b = 150\text{ cm}^2/\text{min}$ . In both cases, the obtained isotherms were identical.

#### Surface potential ( $\Delta_V$ )-surface area ( $A$ ) measurements

The surface potential was measured at the air-water interface by using a gold-coated  $^{241}\text{Am}$  ionising electrode, a reference electrode and an electrometer KP511 (Kriona, Bulgaria), connected to a PC provided with a user software for real-time data measurement. The compression rate was  $U_b = 150\text{ cm}^2/\text{min}$ . The accuracy of the initial surface potential  $\Delta_{V_0}$  measurement was  $\pm 15\text{ mV}$ . However, the accuracy of the rate of surface potential variation  $d\Delta_V/dt$  was  $1\text{ mV/s}$ . As usual, the surface potential of the pure aqueous surface fluctuated during  $\sim 30\text{ min}$ . Then the surface potential became constant and spreading of the monolayer could be performed.

#### Spectrophotometric and isotherm measurements of PAA-monolayers with different ratios of the enol and keto monomer units

(i) The samples (2 ml of PAA solution with  $C_{\text{PAA}} = 2.5 \times 10^{-3}\text{ mg/ml}$ ) were thermostated at  $20 \pm 0.5^\circ\text{C}$  in a quartz-glass cuvette and irradiated with monochromatic (254 nm) UV light under standard conditions. The photochemical reaction was carried out on the setup using a medium pressure mercury lamp (Narva) as the light source in the combination with the IR filter.

The UV absorption spectra were measured on a Specord UV-Vis spectrophotometer.

(ii) The samples (2 ml of PAA solution with  $C_{\text{PAA}} = 0.5\text{ mg/ml}$ ) were irradiated at intervals of 15 min following the above described procedure. After irradiation, the solutions were spread at the air-water interface and the isotherms of the surface pressure were measured.

#### Measurements of the surface area at constant surface pressure during the photochemical reaction at the air-water interface

PAA monolayer was spread on an aqueous subphase in a Teflon rectangular trough ( $6\text{ cm} \times 25\text{ cm} \times 0.7\text{ cm}$ ). After monolayer compression close to the state of maximum packed polymer units, the barostat setup was switched on to maintain the monolayer at constant surface pressure  $\pi = 10\text{ mN/m}$ . The PAA monolayer was then exposed to monochromatic (254 nm) irradiation by using the same light source. The lamp was fixed above the monolayer at a distance of 10 cm in order to irradiate the whole surface area (Fig. 2). The irradiation intensity was measured to be  $1.29 \times 10^{-16}\text{ [quanta s}^{-1}\text{ cm}^{-2}]$ . The irradiation duration was in time intervals of 1–5 min. The increase of the surface area with time was measured. All experiments were

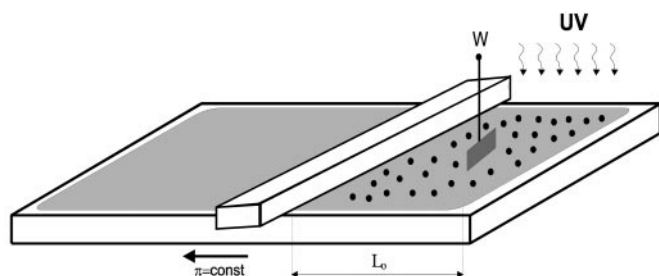


**Fig. 2** Schematic representation of the barostat surface balance for measuring the increase of the surface area during the photochemical reaction of enol–keto tautomerization of PAA monolayers spread at the air–water interface.  $W$  – Wilhelmy plate.  $L_0$  – the length of the monolayer

temperature controlled in order to avoid any artifacts due to the temperature effects. The observed increased surface area versus time was related to the kinetics of the interfacial reorganization of the monolayer induced by the photochemical tautomerization.

#### Molecular models

Molecular models were performed by using the PCMODEL software (Serena software). The force field used in PCMODEL is called MMX and is derived from the MM2 (QCPE-395, 1977) force field of N.L. Allinger, with the pi-VESCF routines taken from MMP1 (QCPE-318) also by N.L. Allinger. The program gives the structure of the monomer units. The monomers are situated at the air–water interface taking into account their hydrophilic–hydrophobic balance.

### Results and discussions

#### Surface pressure and surface potential measurements at the air–water interface

The surface pressure (curve 1) and surface potential (curve 2) isotherms are presented in Fig. 3.

The inflection point observed at about  $14 \text{ \AA}^2/\text{monomer}$  in the surface pressure–surface area isotherm corresponds to closely packed monomers according to the area occupied by an enol acryloylacetone unit. The flat plateau occurring at  $\pi = 18\text{--}19 \text{ mN/m}$  is interpreted as a phase transition and formation into an adjacent phase of the tridimensional structures that could be constituted of both expelled portion (loops) and whole molecules [11]. In our previous studies [9, 10], we assumed that association of

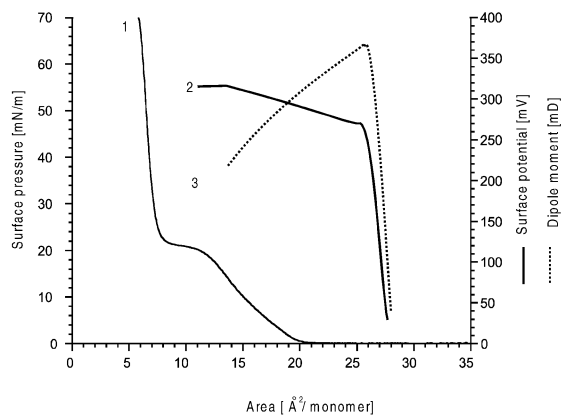


**Fig. 3** Surface pressure ( $\pi$ ) (curve 1); surface potential ( $\Delta_V$ ) (curve 2) and dipole moment ( $\mu$ ) (curve 3) vs. area per enol monomer unit ( $A$ )

the enol units in 3D-structures was related to the formation of hydrogen bonds between monomer units.

The surface potential–area isotherm (curve 2) has three branches corresponding to a large (between 27 and  $25 \text{ \AA}^2/\text{monomer}$ ) and a small (between 25 and  $14 \text{ \AA}^2/\text{monomer}$ ) increase of the surface potential with area, and saturation (below  $14 \text{ \AA}^2/\text{monomer}$ ). The saturation of the surface potential appears at  $14 \text{ \AA}^2/\text{monomer}$ , confirming the closely packed enol acryloylacetate units at the inflection point.

The sum of the vertical components of dipole moments –  $\mu$  of the chemical bonds in one polymer residue are calculated by applying the Helmholtz equation:

$$\Delta_V = 4\pi \frac{\mu}{\epsilon A}, \quad (1)$$

where  $\mu$  is the sum of the vertical components of the dipole moments,  $\epsilon$  is the permittivity and  $A$  is the area of one monomer unit. The permittivity is taken constant and equal to permittivity of polyethylene chains in the bulk phase ( $\epsilon = 2$ ) [12, 13].

In principle, linear polymers take a conformation at the interface in which the main chain backbone lies along the interface and the shorter side chains tend to orient so that their polar parts interact predominantly with the aqueous phase and the nonpolar ones with the non-aqueous phase [11].

Following that concept a possible disposition of the polymer molecule could be proposed (Fig. 4). The main chain backbone as well as the side chains are situated at the air–water interface and the carbonyl and enol groups are anchored to the aqueous phase (Fig. 4A). The enolization affects predominantly the carbonyl groups adjacent to the main polymer chain [3].  $\mu$  can be obtained by using

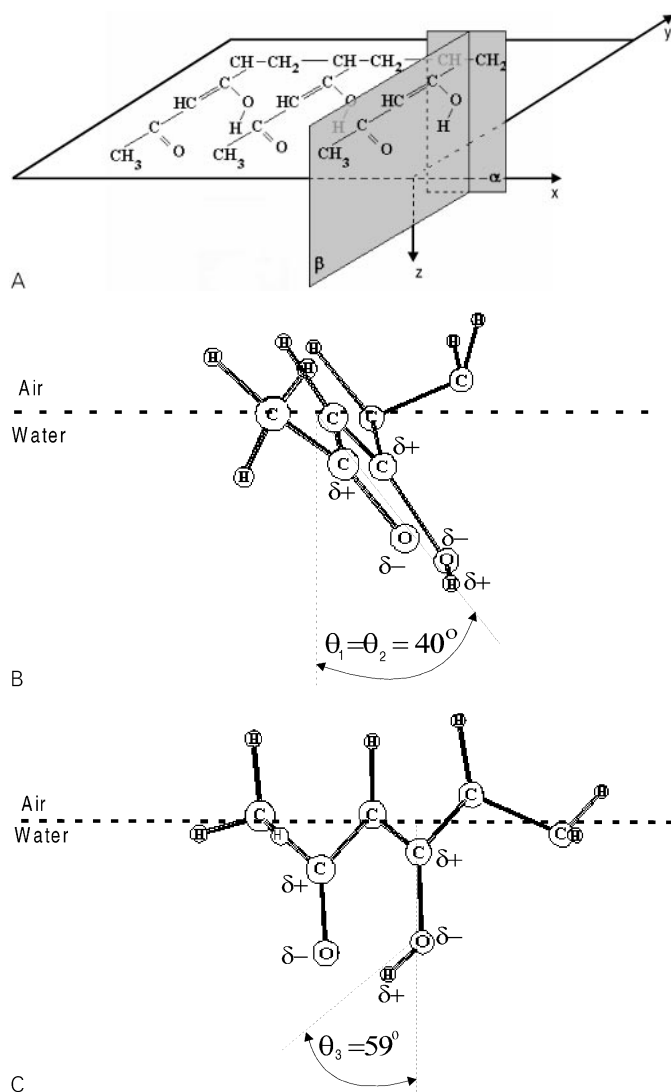


**Fig. 4** Possible disposition of a part of a polymer molecule PAA at the air–water interface.  $\alpha$  and  $\beta$  are two perpendicular plane sections to the plane of interface. Both the main chain backbone, lying in the plane  $\alpha$ , and shorter side chain, lying in the plane  $\beta$  are oriented at the surface in a way that enol and carbonyl groups are anchored to water phase. (A) Perspective drawing of a part of polymer molecule with three polymer residues. (B) Point of view along  $y$  direction towards plane  $\alpha$ . (C) Point of view along  $x$  direction towards plane  $\beta$ . That state corresponds to maximal value of  $\mu$  equal to 362 mD (see the text)

the following expression:

$$\mu = \mu_{C=O} \cos \theta_1 + \mu_{C-O} \cos \theta_2 - \mu_{O-H} \cos \theta_3, \quad (2)$$

where  $\theta_1, \theta_2$  are the angles between normal line of the surface and each of the C=O and C–O groups (Fig. 4B) and  $\theta_3$  is the angle between normal line of the surface and –O–H group (Fig. 4C). Using the data for the dipole moments of the single bounds [14] –  $\mu_{C=O} = 433$  mD,

$\mu_{C-O} = 378$  mD,  $\mu_{O-H} = 487$  mD, and the values of  $\theta_1 = \theta_2 = 40^\circ$  and  $\theta_3 = 59^\circ$ , we obtain for  $\mu$  the value:

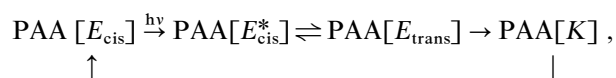
$$\mu = 433 \cos 40^\circ + 378 \cos 40^\circ - 487 \cos 59^\circ \approx 371 \text{ mD}.$$

The large increase of the surface potential from 50 to 265 mV between the areas of 27 and  $25 \text{ \AA}^2/\text{monomer}$  corresponds to an increase of  $\mu$  from 60 to 362 mD (curve 3 in Fig. 3). The maximum value of  $\mu = 362$  mD is in good agreement with the theoretically obtained  $\mu = 371$  mD. This situation corresponds to that state of the monolayer when the main chain backbone as well as the shorter side chains are situated at the air–water interface. The further compression of the monolayer from 25 to  $14 \text{ \AA}^2/\text{monomer}$  leads to a slower increase of the surface potential and to a decrease of the dipole moment. The surface potential reaches the saturation value of 310 mV and corresponding value of the dipole moment of 220 mD. We assumed that during the compression of the monolayer below values of  $25 \text{ \AA}^2/\text{monomer}$  the terminal  $\text{CH}_3$  group of the shorter side chain of the polymer starts to dip in the aqueous phase. The decrease of the dipole moment is then due to the another angle  $\varphi$  between the normal line of the surface and the carbonyl group (Fig. 5). Then, from the experimental value of the dipole moment equal to 220 mD, we can estimate  $\varphi$ :

$$220 = 433 \cos \varphi + 378 \cos 40^\circ - 487 \cos 59^\circ, \quad \varphi = 65^\circ.$$

#### Kinetics of photochemical tautomerization of PAA monolayers

The complete kinetics scheme of the photochemical reaction analyzed in bulk solution of organic solvent [6] and polymer film [7] is:

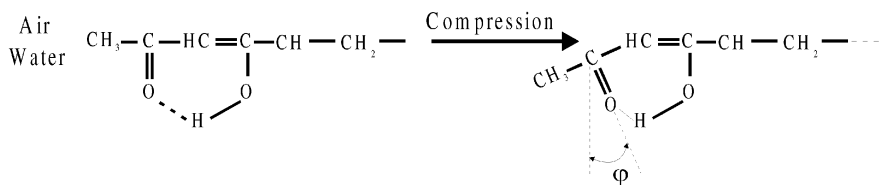


where  $\text{PAA} [E_{\text{cis}}]$ ,  $\text{PAA} [E_{\text{cis}}^*]$ ,  $\text{PAA} [E_{\text{trans}}]$  are the different energetic and isomeric states of the enol form of PAA, and  $\text{PAA} [K]$  is the keto form.

The transformations between  $\text{PAA} [E_{\text{cis}}]$ ,  $\text{PAA} [E_{\text{cis}}^*]$  and  $\text{PAA} [E_{\text{trans}}]$  forms are very fast in comparison with the characteristic time of the monolayer experiment of order of magnitude of 5 min. Then, the conversion between the above forms cannot be detected by the measured interfacial parameter (the change of the surface area) and consequently  $\text{PAA} [E_{\text{cis}}]$ ,  $\text{PAA} [E_{\text{cis}}^*]$  and  $\text{PAA} [E_{\text{trans}}]$  are indistinguishable.

On the other hand, the thermal re-enolization  $\text{PAA} [K] \rightarrow \text{PAA} [E_{\text{cis}}]$  is slower as compared to ketonization  $\text{PAA} [E_{\text{cis}}] \rightarrow \text{PAA} [K]$  and can be neglected. In fact, the

**Fig. 5** Schematic view of the dipping of a terminal CH<sub>3</sub> group of the shorter chain during compression of the monolayer of PAA after the values of the area 25 Å<sup>2</sup>/monomer



characteristic lifetime of dicarbonyl form is of the order 1 h in a dilute bulk solution of organic solvent [6] and several hours in polymer films [7]. It should be mentioned that in the case of a monolayer spread on the water, the polar substrate favours and stabilizes additionally the diketo unit formation.

In order to adapt the kinetics scheme for PAA monolayers, two subsequent stages are considered. The first one is a photochemical transformation of the enol  $[E]$  to keto  $[K]$  form of PAA and the second one is a reorganization of the keto form to more favourable  $[K_i]$  at the interface:



The corresponding kinetics equations are:

$$\begin{aligned} \frac{d\Gamma_K}{dt} &= k_1\Gamma_E - k_2\Gamma_K + k_3\Gamma_{K_i}, \\ \frac{d\Gamma_E}{dt} &= -k_1\Gamma_E, \end{aligned} \quad (4)$$

together with the mass balance equation:

$$\Gamma_E^0 = \Gamma_E + \Gamma_K + \Gamma_{K_i} \quad (5)$$

where  $\Gamma_E$ ,  $\Gamma_K$  and  $\Gamma_{K_i}$  are the surface concentrations, expressed as monomers per unit area of the forms  $E$ ,  $K$  and  $K_i$ , respectively.  $k_1$ ,  $k_2$ ,  $k_3$  are the corresponding rate constants and  $\Gamma_E^0$  is the initial surface concentration of enol units of PAA.

Integration of the Eq. (4) gives

$$\begin{aligned} \Gamma_E(t) &= \Gamma_E^0 e^{-k_1 t}, \\ \Gamma_K(t) &= -\frac{k_1 k_2 \Gamma_E^0}{(k_2 + k_3 - k_1)(k_2 + k_3)} e^{-(k_2 + k_3)t} \\ &\quad + \frac{(k_1 - k_3)\Gamma_E^0}{k_2 + k_3 - k_1} e^{-k_1 t} + \frac{k_3 \Gamma_E^0}{k_2 + k_3}, \\ \Gamma_{K_i}(t) &= \frac{k_1 k_2 \Gamma_E^0}{(k_2 + k_3 - k_1)(k_2 + k_3)} e^{-(k_2 + k_3)t} \\ &\quad - \frac{k_2 \Gamma_E^0}{k_2 + k_3 - k_1} e^{-k_1 t} + \frac{k_2 \Gamma_E^0}{k_2 + k_3}. \end{aligned} \quad (6)$$

The interpretation of the experimental data on the basis of Eq. (6) is a difficult task. Two useful approximations may be developed by the supposition that the photochemical conversion ( $E \rightarrow K$ ) is faster than the interfacial reorganization of the reaction product ( $K \rightleftharpoons K_i$ ).

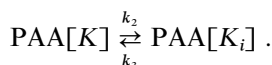
(i) During the time of irradiation  $\tau_{\text{irr}}$  we neglect the reorganization process. The corresponding kinetic system is:

$$\begin{aligned} \text{PAA}[E] &\xrightarrow{k_1} \text{PAA}[K], \\ \Gamma_E(t) &= \Gamma_E^0 e^{-k_1 t}, \end{aligned} \quad (7.1)$$

$$\Gamma_K(t) = \Gamma_E^0 - \Gamma_E(t), \quad (7.2)$$

$$\Gamma_{K_i}(t) = \Gamma_E^0 (1 - e^{-k_1 t}). \quad (7.3)$$

(ii) After irradiation only the reorganization process is taken into account:



The corresponding kinetics and mass-balanced equations are

$$\begin{aligned} \frac{d\Gamma_K}{dt} &= -k_2\Gamma_K + k_3\Gamma_{K_i}, \\ \Gamma^0 &= \Gamma_K + \Gamma_{K_i}, \end{aligned} \quad (8)$$

where  $\Gamma^0$  is the initial concentration of the keto and the reorganized keto units at the interface, obtained during the irradiation. Then

$$\begin{aligned} \Gamma_K(t) &= \frac{k_3}{k_2 + k_3} \Gamma^0 (1 - e^{-(k_2 + k_3)t}) + \Gamma_K^0 e^{-(k_2 + k_3)t}, \\ \Gamma_{K_i}(t) &= \frac{k_3}{k_2 + k_3} \Gamma^0 \left( \frac{k_2}{k_3} + e^{-(k_2 + k_3)t} \right) - \Gamma_K^0 e^{-(k_2 + k_3)t}. \end{aligned} \quad (9)$$

For the first stage  $E \rightarrow K$  we could not determine the kinetics constant  $k_1$  from the direct spectrophotometric experiment at the interface but we could estimate it from the increase of the surface area during irradiation. The experimental data of the increase of the surface area during (with irradiation times  $\tau_{\text{irr}} = 1, 3$  and 5 min) and after the irradiation are presented in Fig. 6.

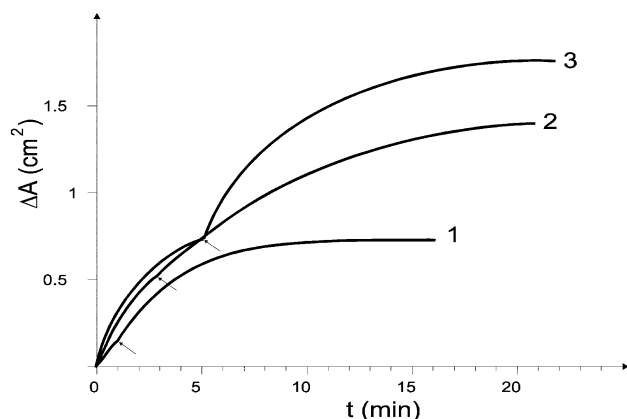


**Fig. 6** Increase of the surface area ( $\Delta A$ ) with time ( $t$ ) at constant surface pressure  $\pi = 5.6$  mN/m during and after the irradiation of a PAA monolayer spread at the air–water interface. The start of irradiation is at  $t = 0$ . The arrows show the stop of the irradiation at  $\tau_{\text{irr}}$ :  $\tau_{\text{irr}} = 1$  min (curve 1);  $\tau_{\text{irr}} = 3$  min (curve 2);  $\tau_{\text{irr}} = 5$  min (curve 3). The bars correspond to the maximal deviation of experimental data. The initial area is  $30 \text{ cm}^2$

In principle, the increase of  $A$  is related to the increase of the area per monomer units during the consecutive conversion of  $E$  into  $K$  and  $K$  into  $K_i$ .

Thus, for the first stage – photoconversion ( $E \rightarrow K$ ):

$$\frac{\Delta A}{A_0} = a_K \Gamma_K - a_E \Gamma_K \quad (10)$$

and by using Eq. (7.2)

$$\frac{\Delta A}{A_0} = (a_K - a_E) \Gamma_E^0 (1 - e^{-k_1 t}), \quad (11)$$

where  $a_E$  and  $a_K$  are surface areas per monomer unit of the enol and keto forms, respectively;  $\Delta A$  is the increase of the surface area measured at constant surface pressure;  $A_0$  is the initial surface area of the monolayer;

Equation (11) fits experimental data  $\Delta A(t)/A_0$  obtained with irradiation times –  $\tau_{\text{irr}} = 1$  min with  $k_1 = 0.84 \text{ min}^{-1}$ ,  $\tau_{\text{irr}} = 3$  min with  $k_1 = 0.70 \text{ min}^{-1}$  and  $\tau_{\text{irr}} = 5$  min with  $k_1 = 0.50 \text{ min}^{-1}$  (data not shown). The value of  $k_1 = 0.84 \text{ min}^{-1}$  obtained at sufficiently short time  $\tau_{\text{irr}} = 1$  min of irradiation corresponds better to the approximation (i).

On the other hand, we determined  $k_1$  from spectrophotometric measurements in the bulk phase of PAA molecular solutions in chloroform in order to compare the process  $E \rightarrow K$  occurring at the interface and in the bulk solution.

The adsorption spectra of PAA show an intense band in the 270–276 nm region. According to [6], the high intensity band at 274 nm is associated with the  $n-\pi^*$

transition in the C–O conjugated ethylene system (enol form). The UV-irradiation of PAA in chloroform at 254 nm resulted in changes of the absorption spectra (Fig. 7). The light induced spectral changes are clearly due to enol  $\rightarrow$  keto conversion. The extinction coefficient of the keto form is very small and therefore only alterations in the concentration of the enol form could be followed spectrophotometrically.

From the experimental data, by applying the simple kinetic model (i) to the conversion  $E \rightarrow K$  in the bulk phase, the rate constant of the reaction ( $E \rightarrow K$ ) is determined to be  $k_1 = 0.28 \text{ min}^{-1}$  (Fig. 8).

The comparison of the rate constants of the photo-induced tautomerization  $E \rightarrow K$  occurring at the interface ( $k_1 = 0.84 \text{ min}^{-1}$ ) and in the bulk solution ( $k_1 = 0.28 \text{ min}^{-1}$ ) shows that the process is approximately 3 times faster if it is organized at the interface when the optimal conditions are realized. In order to relate the photoconversion occurring in a bulk solution to the interfacial properties, the surface pressure–area isotherms of the PAA-monolayers are measured after spreading of a non-irradiated of PAA solution as well as the same solution irradiated for 15 and 30 min. The results are given in Fig. 9.

Curve 1 represents isotherm of the PAA before the photochemical conversion, where the enol form is predominant – 96% [6, 7]. We have assumed in our previous studies that the nature of the observed flat plateau is related to the creation of hydrogen bonds between enol units leading to a 2D  $\rightarrow$  3D phase transition [9, 10]. Between keto units there is no hydrogen interaction and the phase transition disappears progressively as a result of the photoconversion  $E \rightarrow K$  (curves 2 and 3).

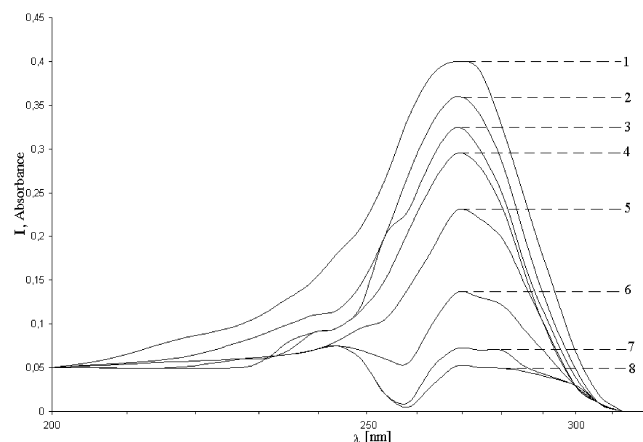


**Fig. 7** UV-spectra of PAA in  $\text{CHCl}_3$  ( $C_{\text{PAA}} = 2.5 \times 10^{-3} \text{ mg/ml}$ ) measured at different irradiation times  $\tau_{\text{irr}}$ : non-irradiated (1);  $\tau_{\text{irr}} = 0.2$  min (2);  $\tau_{\text{irr}} = 0.5$  min (3);  $\tau_{\text{irr}} = 0.8$  min (4);  $\tau_{\text{irr}} = 1.8$  min (5);  $\tau_{\text{irr}} = 3.8$  min (6);  $\tau_{\text{irr}} = 5.8$  min (7);  $\tau_{\text{irr}} = 7.8$  min (8)

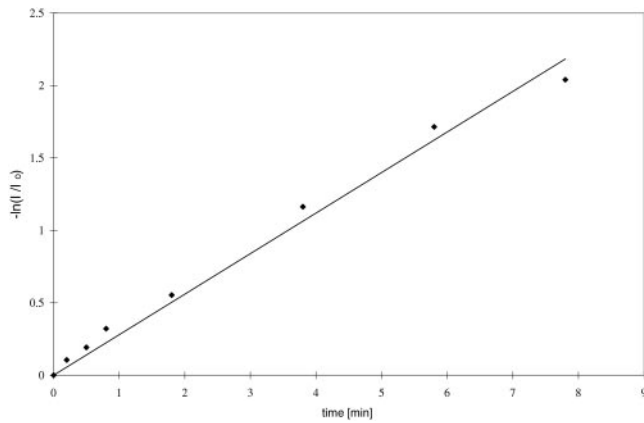


**Fig. 8** Fit of the experimental data from Fig. 7 using the kinetic model for enol to keto conversion

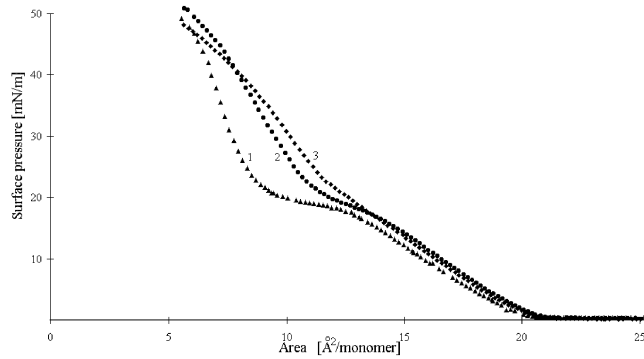


**Fig. 9** Surface pressure ( $\pi$ )–area per monomer unit ( $A$ ) obtained after spreading of a solution of PAA ( $C_{\text{PAA}} = 0.5 \text{ mg/ml}$ ) irradiated at different duration: without irradiation  $\tau_{\text{irr}} = 0 \text{ min}$  (curve 1);  $\tau_{\text{irr}} = 15 \text{ min}$  (curve 2);  $\tau_{\text{irr}} = 30 \text{ min}$  (curve 3)

For the second stage – reorganization of the keto form ( $K \rightleftharpoons K_i$ ):

$$\frac{\Delta A}{A_0} = a_{K_i}(\Gamma_{K_i} - \Gamma_{K_i}^0) - a_K(\Gamma_K^0 - \Gamma_K), \quad (12)$$

where  $a_K$  and  $a_{K_i}$  are surface areas per monomer unit of the keto and the reorganized at the interface keto forms, respectively;  $\Gamma_K^0$  and  $\Gamma_{K_i}$  are the surface concentrations at time  $\tau_{\text{irr}}$  of the keto form and the already reorganized at the interface keto form, respectively.

After substitution of Eq. (9) into Eq. (12), we obtain

$$\frac{\Delta A}{A_0} = b_1 + b_2 e^{-b_3 t}, \quad (13)$$

where

$$b_1 = (a_K k_3 + a_{K_i} k_2) \frac{1}{k_2 + k_3} \Gamma^0 - a_K \Gamma_K^0 - a_{K_i} \Gamma_{K_i}^0,$$

$$b_2 = (a_{K_i} - a_K) \left( \frac{k_3}{k_2 + k_3} \Gamma^0 - \Gamma_K^0 \right),$$

$$b_3 = k_2 + k_3. \quad (14)$$

From the fit of the experimental data after irradiation, Fig. 6 and Eq. (13), we can determine  $b_3 = k_2 + k_3 = 0.32 \text{ min}^{-1}$ .

The increase of the areas during the consecutive conversion of  $E$ ,  $K$  and  $K_i$  can be estimated for a short irradiation time ( $\tau_{\text{irr}} = 1 \text{ min}$ ).

Equation (11) gives for  $t = \tau_{\text{irr}}$ :

$$\frac{\Delta A_{\tau_{\text{irr}}}}{A_0} = (a_K - a_E) \Gamma_{K(t=\tau_{\text{irr}})}. \quad (15)$$

From the area of  $14 \text{ Å}^2/\text{monomer}$  of closely packed enol units (Fig. 3, curve 1) and taking into account that before irradiation, the enol form predominates (96%), for the initial concentration of the enol form we obtain:

$$\Gamma_E^0 = (1/14) \times 0.96 \times 10^{16} = 6.86 \times 10^{14} [\text{monomer}/\text{cm}^2].$$

In order to estimate the concentration of the keto form –  $\Gamma_{K(t=\tau_{\text{irr}})}$  after irradiation during the short interval of 1 min we use the Eq. (7.3) with

$$t = 1 \text{ min} \quad k_1 = 0.84 \text{ min}^{-1} \quad \text{and}$$

$$\Gamma_E^0 = 6.86 \times 10^{14} [\text{monomer}/\text{cm}^2]$$

and obtain:

$$\Gamma_K^0 = 3.9 \times 10^{14} [\text{monomer}/\text{cm}^2].$$

From experimental data  $\Delta A_{\tau_{\text{irr}}} = 0.125 \text{ cm}^2$  (Fig. 6, curve 1) and  $A_0 = 30 \text{ cm}^2$ .

With the values of  $A_0$ ,  $\Delta A_{\tau_{\text{irr}}}$  and  $\Gamma_{K(t=\tau_{\text{irr}})}$ , and Eq. (15) the increase of the area of one unit resulting from the photoconversion of enol to keto form is

$$a_K - a_E = 0.11 \text{ Å}^2. \quad (16)$$

For short irradiation times ( $\sim \tau_{\text{irr}} = 1 \text{ min}$ ), the approximation (i) is reasonable and the initial surface concentration of keto form is  $\Gamma^0 = \Gamma_K^0 = \Gamma_{K(t=\tau_{\text{irr}})}$ , while  $\Gamma_{K_i}^0 = 0$ , then Eq. (13) can be simplified. At the end of the process ( $t \rightarrow \infty$ ) Eq. (13) can be written as

$$\frac{\Delta A_{\infty}}{A_0} = (a_{K_i} - a_K) \frac{k_2}{k_2 + k_3} \Gamma_K^0 \quad (17)$$

and with the evident relationships

$$0 < \frac{k_2}{k_2 + k_3} < 1,$$

$$0 < k_2 < 0.3. \quad (18)$$

Equation (17) becomes

$$\frac{\Delta A_{\infty}}{A_0} > (a_{K_i} - a_K) \Gamma_K^0. \quad (19)$$

From the experimental data  $\Delta A_\infty = 0.75 \text{ cm}^2$  (Fig. 6, curve 1) and  $A_0 = 30 \text{ cm}^2$ . After the substitution of values for  $\Delta A_\infty$ ,  $A_0$  and  $\Gamma_K^0$  in Eq. (19) we obtained a reasonable estimation of the increase of the area of one unit, resulting from the interfacial reorganization of the keto form:

$$a_{K_i} - a_K < 1.50 \text{ \AA}^2. \quad (20)$$

In conclusion, a simple well-defined system – PAA monolayer is used in the present study as a tool for the investigation of the mechanism and kinetics of the

photochemical enol–keto tautomerization at the interface. The molecular interpretation of the increase of the areas is a difficult task and likely some different approach has to be applied, for example, conformation analysis based on the computer simulation.

In the future we intend to compare the mechanism of this reaction occurring in variously organised media as monolayers, multilayers or dispersions.

**Acknowledgements** This work was partly supported by the Bulgarian National Foundation for Scientific Research Projects.

## References

1. Tomida T, Tomida M, Nishihara Y, Nakabayashi I, Okazaki T, Masuda S (1990) *Polymer* 31:102
2. Petkov I, Masuda S, Sertova N, Grigorov L (1995) *Photochem Photobiol A: Chem* 85:191
3. Masuda S, Tanaka M, Ota T (1989) *J Polym Sci: Part A: Polym Chem* 27:855
4. Masuda S, Tanaka M, Minagawa K, Asahi Y (1992) *Pre Appl Chem JMS A* 29:821
5. Arnaut LG, Formosinho SJ (1993) *J Photochem Photobiol A: Chem* 75:1
6. Petkov I, Masuda S, Sertova N, Grigorov L (1996) *J Photochem Photobiol A: Chem* 95:189
7. Masuda I, Sertova SN, Petkov I (1997) *J Polym Sci: Part A: Polym Chem* 35:3683
8. Petty M, Bryce M, Bloor D (1995) *Introduction to Molecular Electronics*. Edward Arnold, St. Edmundsbury Press Ltd
9. Balashev K, Panaiotov I, Petkov I, Proust JE, Masuda S (1997) *J Dispersion Sci Technol* 18(6 & 7):661
10. Balashev K, Bois A, Proust JE, Ivanova Tz, Petkov I, Masuda S, Panaiotov I (1997) *Langmuir* 13:5362–6367
11. Mac Ritchie (1990) *Chemistry at Interfaces*. Academic press, San Diego
12. Davies JT, Rideal E (1961) *Interfacial Phenomena*. Academic Press, New York
13. Gaines GL (1969) *Insoluble Monolayers at Liquid–Gas Interfaces*. Wiley Interscience, New York
14. Markov P (1982) Thesis, University of Sofia